Structural Characterization of the Interaction of the δ and α Subunits of the *Escherichia coli* F_1F_0-ATP Synthase by NMR Spectroscopy[†,‡]

Stephan Wilkens,*[,§] Dan Borchardt,[||] Joachim Weber,[⊥,#] and Alan E. Senior[⊥]

Departments of Biochemistry and Chemistry, University of California at Riverside, Riverside, California 92521, and Department of Biochemistry and Biophysics, University of Rochester Medical Center, Box 712, Rochester, New York 14642

Received June 6, 2005; Revised Manuscript Received July 11, 2005

ABSTRACT: A critical point of interaction between F_1 and F_0 in the bacterial F_1F_0-ATP synthase is formed by the α and δ subunits. Previous work has shown that the N-terminal domain (residues 3−105) of the δ subunit forms a 6 α-helix bundle [Wilkens, S., Dunn, S. D., Chandler, J., Dahlquist, F. W., and Capaldi, R. A. (1997) *Nat. Struct. Biol. 4*, 198−201] and that the majority of the binding energy between δ and F_1 is provided by the interaction between the N-terminal 22 residues of the α- and N-terminal domain of the δ subunit [Weber, J., Muharemagic, A., Wilke-Mounts, S., and Senior, A. E. (2003) *J. Biol. Chem. 278*, 13623−13626]. We have now analyzed a 1:1 complex of the δ-subunit N-terminal domain and a peptide comprising the N-terminal 22 residues of the α subunit by heteronuclear protein NMR spectroscopy. A comparison of the chemical-shift values of δ-subunit residues with and without α N-terminal peptide bound indicates that the binding interface on the N-terminal domain of the δ subunit is formed by α helices I and V. NOE cross-peak patterns in 2D $^{12}C/^{12}C$-filtered NOESY spectra of the ^{13}C-labeled δ-subunit N-terminal domain in complex with unlabeled peptide verify that residues 8−18 in the α-subunit N-terminal peptide are folded as an α helix when bound to δ N-terminal domain. On the basis of intermolecular contacts observed in $^{12}C/^{13}C$-filtered NOESY experiments, we describe structural details of the interaction of the δ-subunit N-terminal domain with the α-subunit N-terminal α helix.

F_1F_0-ATP synthase is a large multisubunit enzyme complex found in the mitochondrial and bacterial inner membrane and the thylakoid membrane of chloroplasts (*1*−*3*). The *Escherichia coli* complex is organized into two functional domains, a cytoplasmic soluble portion of the F_1F_0-ATP synthase (F_1)[1] containing subunits $\alpha\beta\gamma\delta\epsilon$ in a ratio of 3:3:1:1:1 and a membrane-bound F_0, which is made of one *a*, two *b*, and a ring of 10 *c* subunits. Synthesis or hydrolysis of ATP is catalyzed by the β subunits of the F_1, and this process is coupled to ion translocation through the membrane-bound F_0. The F_1 and F_0 domains are joined by two stalks, a central one, composed of subunits γ and ε, and a peripheral one, composed of subunits *b* and δ (subunit nomenclature of the bacterial enzyme). F_1F_0-ATP synthase is a rotary motor enzyme. The potential energy of the electrochemical gradient released in the membrane spanning F_0 is consumed on the F_1 for net synthesis of ATP, and the coupling of these two processes involves a rotation of the central stalk within the catalytic core formed by the alternating α and β subunits of the F_1. The peripheral stalk, composed of the F_1 δ subunit and the F_0 *b* subunits, acts as a stator holding the F_1 and F_0 in the correct spatial arrangement for energy coupling to occur. X-ray crystallographic models are available for the F_1 from mammalian mitochondria, chloroplast, and the thermophilic bacterium PS3 (*4*−*8*). None of these structures, however, contains information about the structure of the stator domain or its interaction with the α and β subunits of the F_1.

Previously, we have reported structural features of the *E. coli* δ subunit by solution nuclear magnetic resonance (NMR) spectroscopy (*9*). The data showed that the δ subunit is a two-domain protein with a stable N-terminal domain (residues 2−106), folded as a six-helix bundle, and a C-terminal domain (residues 107−177), which appeared to be largely unstructured in solution. When electron microscopic images of the intact F_1F_0-ATP synthase decorated with a monoclonal antibody directed against the δ subunit were analyzed, we could show that a large domain of the δ subunit binds on the very top of the F_1 domain, near the N termini of the α and β subunits (*10*), thereby confirming earlier biochemical (*11*−*12*), genetic (*13*), and chemical cross-linking (*14*−*16*) data, which had indicated that the N termini of the α subunits are important for the interaction of the δ subunit with the

[†] Supported by NIH Grants GM58600 to S.W. and GM25349 to A.E.S.

[‡] The coordinates of the minimized average structure of the αN−δ′ complex have been deposited in the PDB data bank under the accession number 2A7U.

* To whom correspondence should be addressed. Telephone: 951-827-3131. Fax: 951-827-4434. E-mail: stephan.wilkens@ucr.edu.

[§] Department of Biochemistry, University of California at Riverside.

[||] Department of Chemistry, University of California at Riverside.

[⊥] University of Rochester Medical Center.

[#] Current address: Department of Chemistry and Biochemistry, Texas Tech University, Lubbock, Texas 79409.

[1] Abbreviations: F_1, soluble portion of the F_1F_0-ATP synthase; αN, peptide comprising the N-terminal 22 residues of the *E. coli* F_1-ATPase α subunit; δ′, N-terminal 135 residues of the *E. coli* F_1-ATPase δ subunit; δ^{1-106}, N-terminal 106 residues of the *E. coli* F_1-ATPase δ subunit; NMR, nuclear magnetic resonance; NOE, nuclear Overhauser enhancement; NOESY, nuclear Overhauser enhancement spectroscopy; HSQC, heteroatom single-quantum coherence; cosy, correlation spectroscopy; tocsy, total correlation spectroscopy; roesy, rotating-frame Overhauser enhancement spectroscopy.

10.1021/bi0510678 CCC: $30.25
Published on Web 08/09/2005

F_1. Subsequent binding studies revealed that the δ-subunit N-terminal domain was able to bind to the F_1 with similar affinity compared to the full-length subunit (*17*), and in separate studies, it could be shown that the C-terminal domain of δ was required for the interaction with the F_0 *b* subunits (*18*). More recently, it has been reported that a peptide comprising the N-terminal 22 amino acids of the α subunit is able to bind to full-length δ subunit and δ-subunit N-terminal domain with 1:1 stoichiometry and high affinity (*19*). Introducing mutations into the δ subunit and analyzing the binding of the α-subunit N-terminal peptide to the resulting mutant δ subunits suggested that the binding interface between the α N-terminal peptide and δ subunit was formed by δ-subunit helices I and V (*19*). These two helices constitute one face of the δ-subunit N-terminal domain and expose several residues to the solvent (including Tyr11, Ala14, Phe18, Leu76, and Val79), which form a hydrophobic pocket that is lined by hydrophilic and charged residues.

Here, we analyzed complexes of the δ-subunit N-terminal domain with wild-type and mutant α-subunit N-terminal peptides by heteronuclear multidimensional protein NMR spectroscopy. The NMR data verify that the α-subunit N-terminal peptide binds as an α helix to the δ-subunit N-terminal domain and that analysis of intermolecular nuclear Overhauser enhancements (NOEs) reveal structural details of the α−δ subunit interface.

EXPERIMENTAL PROCEDURES

Materials. $^{15}NH_4Cl$ and $^{13}C_6$-glucose were from Isotec, Inc. or Cambridge Isotopes. Uniformly ^{15}N and ^{13}C and ^{15}N-labeled N-terminal 135 residues of the *E. coli* F_1-ATPase δ subunit (δ′) was expressed in *E. coli* strain 594 and purified as described (*9*). The peptide comprising the N-terminal 22 residues of the *E. coli* F_1-ATPase α subunit (called αN in this paper) was prepared by chemical synthesis (*19*). In addition to the "wild-type" α-subunit N-terminal peptide, the following mutants were used in the NMR binding studies: I8E, L11E, and I16E. Biochemical characterization of the interaction of these mutants with the N-terminal domain of δ has been published (*20*).

NMR Spectroscopy: Sample Preparation. Purified δ′ was precipitated by ammonium sulfate and desalted by two consecutive centrifuge columns in 10 mM sodium potassium phosphate buffer at pH 7.2, 3 mM sodium azide, and 0.1 mM EDTA. The wild-type N-terminal peptide of the α subunit was dissolved in the same buffer or water plus 40 mM potassium hydroxide at a concentration of 15 mg/mL (6 mM). Some of the mutant peptides were dissolved in DMSO. For NMR spectroscopy of a 1:1 complex of δ′ and αN-terminal peptide, δ′ was desalted by one centrifuge column, followed by addition between 1.1 and 1.5 times the stoichiometric amount of the αN-terminal peptide. The mixture was incubated for up to 1 h at room temperature, and the resulting complex was passed over a second centrifuge column to remove residual ammonium sulfate and potassium hydroxide or DMSO used to prepare the stock solution of the αN-terminal peptide. For the titration of δ′ with the wild-type α-subunit peptide, a predetermined amount of 200 mM H_3P0_4 was added after the last addition of peptide to readjust the pH to 7.2.

NMR Spectroscopy: Data Collection and Analysis. NMR spectra were recorded on a 11.7 T Varian Inova or a 14 T Bruker AMX NMR spectrometer at temperatures between 18 and 25 °C. A total of 7% (40 μL) deuterium oxide was included in the 600 μL NMR samples for frequency lock. The following NMR experiments were recorded on the Varian Inova (all implemented in the "Protein Pack" of pulse sequences available for the Varian Inova spectrometer): 2D $^1H,^{15}N$-heteroatom single-quantum coherence (HSQC) (gNhsqc); 2D wnoesy, wroesy, wcosy, and wtocsy (in D_2O); 3D $^1H,^{15}N$-nuclear Overhauser enhancement spectroscopy (NOESY)−HSQC (NOESY-gNhsqc); and 2D $^1H,^{13}C$-HSQC (gChsqc). $^{13}C/^{12}C$-filtered 2D NOESY (*21*) was recorded for selective detection of NOEs from protons attached to ^{13}C (δ N-terminal domain) to protons attached to ^{12}C (α-subunit N-terminal peptide). Assignment of α-subunit N-terminal peptide proton resonances was aided by conducting $^{12}C/^{12}C$ and $^{14}N/^{12}C$-filtered 2D NOESY experiments, which selectively detect NOEs within the α-subunit N-terminal peptide only. These spectra were recorded using a double half-filter sequence (*22*, *23*) with a modified phase cycle that directly gave the desired subspectrum. All NMR spectra were analyzed within Felix2000 (Accelrys). Gaussian line broadening or a squared shifted sinebell was used for apodization. The 3D $^1H,^{15}N$-NOESY−HSQC recorded on the Bruker AMX spectrometer was acquired with 1024, 128, and 28 complex points in F3, F2, and F1, respectively, with spectral widths of 8000, 8000, and 3000 Hz. The resonances of the δ-subunit N-terminal domain in the δ′−αN-terminal peptide (wild-type) complex were assigned from the 3D $^1H,^{15}N$-NOESY−HSQC from the sequential NOE cross-peak patterns. Proton resonances were referenced using DSS as an external standard. Nitrogen and carbon resonances were referenced indirectly to DSS via their calculated zero-point frequencies. NOEs were classified as strong (<3 Å), medium (<4 Å), weak (<5 Å), or very weak (<5.5 Å). Structure calculations were done as described in ref *9*.

RESULTS

NMR Spectroscopy of the αN−δ′ Complex. To monitor the formation of the complex between δ′ and αN (δ′−αN), uniformly ^{15}N-labeled δ′ was titrated with αN and 2D $^1H,^{15}N$-HSQC spectra were recorded after the addition of 0.2, 0.4, 0.8, 1.2, and 1.5 equiv of αN to a 0.6 mM solution of ^{15}N-labeled δ′. Figure 1A shows a region of the 2D $^1H,^{15}N$-HSQC spectrum of δ′ recorded in the absence and presence of increasing amounts of αN. The disappearance of the δ′ peaks and the appearance of new peaks with a different chemical-shift value indicated that binding of αN to δ′ occurred with high affinity (slow exchange) and that the resulting complex adopted a defined and stable conformation. Figure 1B shows the overlay of 2D $^1H,^{15}N$-HSQC spectra of δ′ (shown in blue) and the αN−δ′ complex (shown in red). Overall, the spectrum of the complex has a similar appearance compared to the spectrum of δ′ alone, suggesting that the structure of the δ-subunit N-terminal domain does not change significantly upon binding of the α-subunit N-terminal peptide.

Assignment of the δ′ Amide Resonances in the δ′−αN Complex. As can be seen from Figure 1B, almost all of the δ′ amide resonances in the δ′−αN complex were shifted so that, especially in the crowded region of the 2D spectrum, assignment of the amide resonances based on the assignments

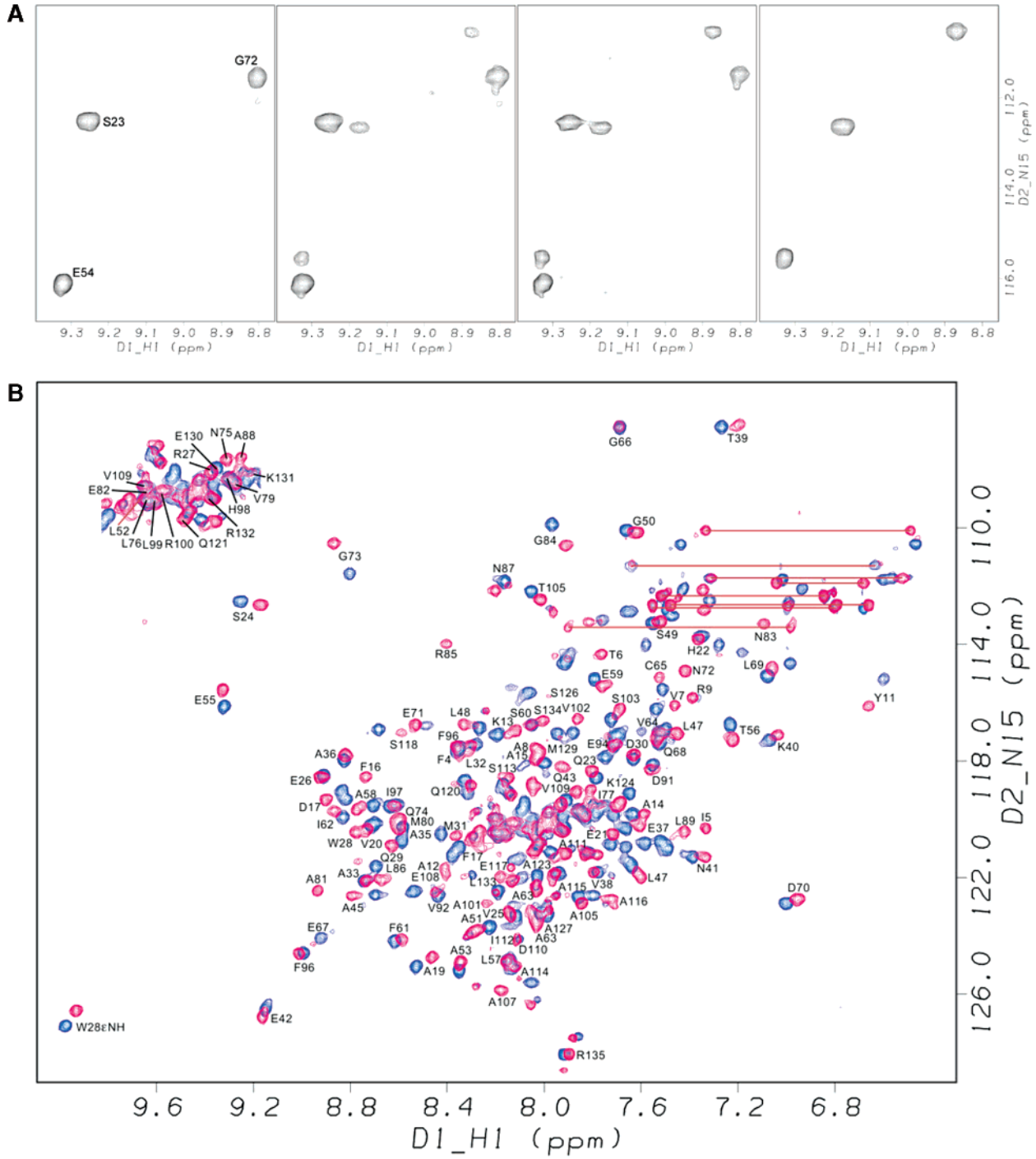

FIGURE 1: Complex formation between δ' and αN as monitored by NMR spectroscopy. (A) Titration of 0.6 mM δ' in 10 mM Na,KP0$_4$ at pH 7.2, 0.1 mM EDTA, and 3 mM NaN_3 with α-subunit N-terminal peptide. Shown are regions of 2D ^{1}H,^{15}N-HSQC spectra before (left spectrum) and after addition of 0.4, 0.8, and 1.5 equiv of peptide, respectively. The appearance of new peaks accompanied by the disappearance of the δ' peaks indicates that the peptide binds with high affinity (slow exchange). After the last addition of peptide, the pH was readjusted to a value of 7.2 to ensure that the observed changes were indeed due to peptide binding. (B) Two-dimensional ^{1}H,^{15}N-HSQC spectra of δ' alone (blue) and δ' in the presence of 1.5 equiv of α N-terminal peptide (red). The spectrum of the αN−δ' complex was recorded after one additional centrifuge column to re-establish the same buffer conditions under which the spectrum of δ' was recorded. The assignments are for δ' residues in complex with α N-terminal peptide. Primary amide protons are indicated by horizontal lines. Note that the residue numbering starts with the missing N-terminal Met at position 1.

obtained for isolated δ' (*9*) was not possible. To "re-assign" the amide resonances of δ' in the δ'−αN complex, 3D ^{1}H,^{15}N-NOESY−HSQC spectra were recorded. A comparison of the 3D spectra of δ' and δ' complexed with αN allowed assignment of essentially all of the shifted δ' amide resonances based on their NOE cross-peak patterns. With few exceptions, NOE cross-peak patterns for δ' residues in the δ'−αN complex were essentially unchanged compared to the NOE cross-peak patterns of the same residues in free δ', again indicating that the three-dimensional structure of δ' does not significantly change upon binding of the α-subunit N-terminal peptide (data not shown).

Binding Site of the α-Subunit N-Terminal Peptide on the δ-Subunit N-Terminal Domain. Figure 2A shows the dif-

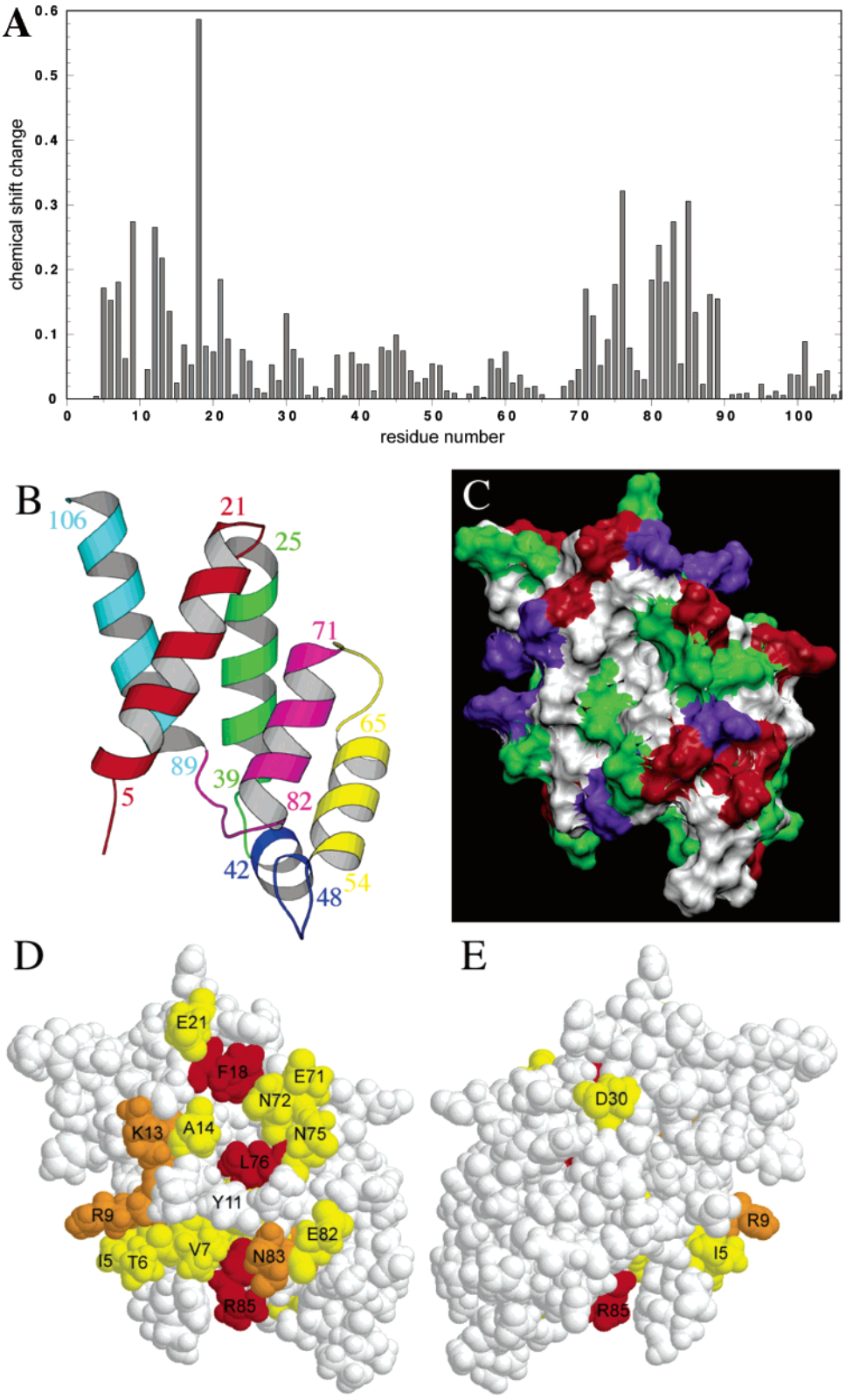

FIGURE 2: Chemical-shift changes of δ′ amide protons upon peptide binding. (A) Proton chemical-shift changes (absolute values) are plotted against the residue number. Chemical shift differences >0.1 ppm were considered significant. (B) Ribbon diagram of the solution structure of the N-terminal 106 residues of the δ subunit (*9*). (C) Surface representation of the same structure with hydrophobic, polar, basic, and acidic residues shown in white, green, blue, and red, respectively. (D and E) Front- and backview of the N-terminal 106 residues of the δ subunit in spacefill. Residues with a peptide-binding-induced chemical-shift change larger than 0.3, 0.2, and 0.1 ppm are in red, orange, and yellow, respectively. In the left image, α helices I and V are in the front. The right image shows the structure rotated by 180° around the vertical. The diagrams shown in A−D were generated in Molscript (*32*), VMD (http://www.ks.uiuc.edu/Research/vmd), and RasMol, respectively.

ferential amide proton chemical shifts of residues 3−106 of δ′ versus the δ′−αN complex. As can be seen, significant chemical-shift changes occur in two regions of the primary sequence of δ′, including residues 4−21 (helix I) and 71−

89 (helix V). δ' residues 107−135, which contain an unstructured linker (residues 107−120) and a poorly structured, solvent-exposed α helix (residues 121−135) show very little change in chemical shift upon binding of αN (not shown). Figure 2B shows the ribbon diagram of the N-terminal 106 residues of the δ subunit (δ^{2-106}) with α helices I and V pointing toward the front. Figure 2C shows the surface representation of δ^{2-106} in the same orientation as in Figure 2B with hydrophobic, polar, and positively and negatively charged residues in white, green, blue, and red, respectively. Parts D and E of Figure 2 show the space-filling models of δ^{2-106} oriented as in Figure 2B (D) and rotated 180° around the vertical (E). Residues with an amide proton chemical-shift change ($\Delta\delta$) of $0.1 < \Delta\delta < 0.2$, $0.2 < \Delta\delta < 0.3$, and $\Delta\delta > 0.3$ ppm are shown in yellow, orange, and red, respectively. As can be seen, all residues with a chemical-shift change greater than 0.1 ppm are located on one face of δ^{2-106}, with the exception of Asp30, which is on the opposite face, in α helix III.

Assignment and Secondary Structure Analysis of α*-Subunit N-Terminal Peptide.* Circular dichroism (CD) measurements reported earlier indicated that the α-subunit N-terminal peptide contained a significant amount of α-helical secondary structure in aqueous solution (*19*). This observation is consistent with secondary structure prediction for the peptide as shown in Figure 3A. To obtain proton resonance assignments for α-subunit N-terminal peptide residues, $^{12}C/^{12}C$-filtered NOESY spectra were recorded (Figure 3B). The relatively small size of the peptide allowed assignment of most of the α and side-chain protons from the 2D spectra. The assignment was started from the two asparagines at positions 4 and 20. Asparagines typically have downfield-shifted α-proton chemical shifts and two strong cross-peaks from the α to its β protons (see Figure 3B). NOE cross-peaks were observed from one of the asparagines to the only aromatic side chain in the peptide (phenylalanine 19). This asparagine also showed cross-peaks to a side chain with resonances typical for a valine, and it was therefore assigned as asparagine 20. The other asparagine showed NOE cross-peaks to a serine (serine 5) and a leucine (leucine 3) and was therefore assigned as asparagine 4. Subsequently, essentially all of the carbon-attached protons from the entire peptide were assigned residue by residue by starting from the two asparagines at the N and C terminus. Some of the overlap, especially in the α−aliphatic and aliphatic−aliphatic proton NOE cross-peak region could be resolved by recording spectra at different temperatures (data not shown). Additional ambiguities could be resolved during the various stages of the structure calculations. Overall, strong NOEs were observed for sequential connectivities, and weaker NOEs were observed for medium range connectivities typical for α-helical secondary structure. Subsequently, NOE cross-peaks were also obtained from $^{14}N/^{12}C$-filtered NOESY experiments recorded in H_2O (data not shown). Probably because of the necessary water suppression, only NOEs for the more flexible C-terminal residues were observed (residues 14 and 17−21). These NOEs were consistent with the assignments obtained from the $^{12}C/^{12}C$-filtered NOESY spectra and were therefore included in the later stages of the structure refinement. Table 1 shows the assignments obtained for the α-subunit N-terminal peptide in complex with the N-terminal domain of the δ subunit. As can be seen, most α-proton resonances (Ser5, Thr6, Ser9, Glu10, Ile12, Lys13, Gln14, Ile16, Ala17, Gln18, Phe19, and Asn20) are shifted upfield by more than 0.1 ppm, indicating that these residues of the α-subunit N-terminal peptide adopt α-helical conformation when bound to δ'. The α-proton resonances of the remaining residues (except Met1 and Val22 for which no assignments were obtained) are either shifted downfield (Leu3, Asn4, Glu7, and Ile8) or are close to their random coil value (Leu11, Arg15, and Val21). On the helical wheel, these residues point to the hydrophilic face of the helix.

Complex formation between the α-subunit N-terminal peptide and δ' led to the appearance of two upfield resonances at −0.02 and −0.34 ppm. The two resonances were not seen in unedited proton NMR spectra of δ' alone and in 2D $^{1}H,^{13}C$-HSQC spectra of a complex between uniformly $^{13}C/^{15}N$-labeled δ' and unlabeled peptide, suggesting that they originate from the α-subunit N-terminal peptide, most likely from one or more of the hydrophobic isoleucine or leucine residues at positions 8, 11, 12, and/or 16. Complexes of the δ N-terminal domain with either α-subunit Ile8Glu or Leu11Glu mutants produced similar amide chemical-shift differences in 2D $^{1}H,^{15}N$-HSQC spectra compared to the wild-type peptide, indicating that these peptides bind in a similar way. Two-dimensional NOESY spectra of δ' with either of these two peptides bound showed that both resonances at −0.02 and −0.34 ppm were still present, suggesting that these resonances belong to Ile12 and Ile16 and that these two isoleucine side chains are contributing most to the binding interaction between the α-subunit N-terminal peptide and δ'. Much smaller amide chemical-shift changes were seen upon complex formation with the mutant peptide Ile16Glu, consistent with its significantly weaker binding as determined by fluorescence (*20*). Nevertheless, complex formation with Ile16Glu produced an upfield resonance located at −0.28 ppm with a NOE cross-peak pattern similar to the −0.34 ppm resonance observed with the wild-type peptide, suggesting that the −0.34 ppm resonance belongs to Ile12 (αN mutant data not shown).

Structure of the α*-Subunit N-Terminal Peptide.* On the basis of the NMR and CD data mentioned above, residues Asn4−Phe19 of the α-subunit N-terminal peptide were modeled as an α helix using short- and medium-range distance and dihedral angle restraints typical for α-helical secondary structure (14 short HN−HN, 13 medium $HN_i-\alpha_{i-1}$, 10 long $\alpha_i-\beta_{i+3}$, and 12 dihedral angles of −60°). A total of 25 structures were calculated using the protocols for template generation, subembedding, distance geometry by simulated annealing, and refinement within the X-PLOR package of programs (*24*). The 25 structures were subsequently averaged, and the average was subjected to energy minimization. At this point in the analysis, unambiguous distance restraints from the $^{12}C/^{12}C$- and $^{14}N/^{12}C$-filtered NOESY experiments were introduced to refine the modeled structure of the α-subunit N-terminal peptide. The resulting structure was used to identify additional NOEs, and the process was iterated until a total of 169 experimental distance restraints were obtained (82 intraresidue, 45 sequential, and 42 medium range). At this stage, 10 structures of the α-subunit N-terminal peptide were calculated from experimental distance restraints only (without the modeled restraints). The 10 structural models were averaged and energy-minimized. The final 10 structures had no NOE violations

A

conf:	9	7	6	5	5	6	6	8	9	9	9	9	9	8	8	8	6	4	1	4	8	9
seq:	M	Q	L	N	S	T	E	I	S	E	L	I	K	Q	R	I	A	Q	F	N	V	V
pred:	C	C	C	C	H	H	H	H	H	H	H	H	H	H	H	H	H	H	H	C	C	C
CSI:		1	-1	-1	1	1	-1	-1	1	1	0	1	1	1	0	1	1	1	1	1	0	

B

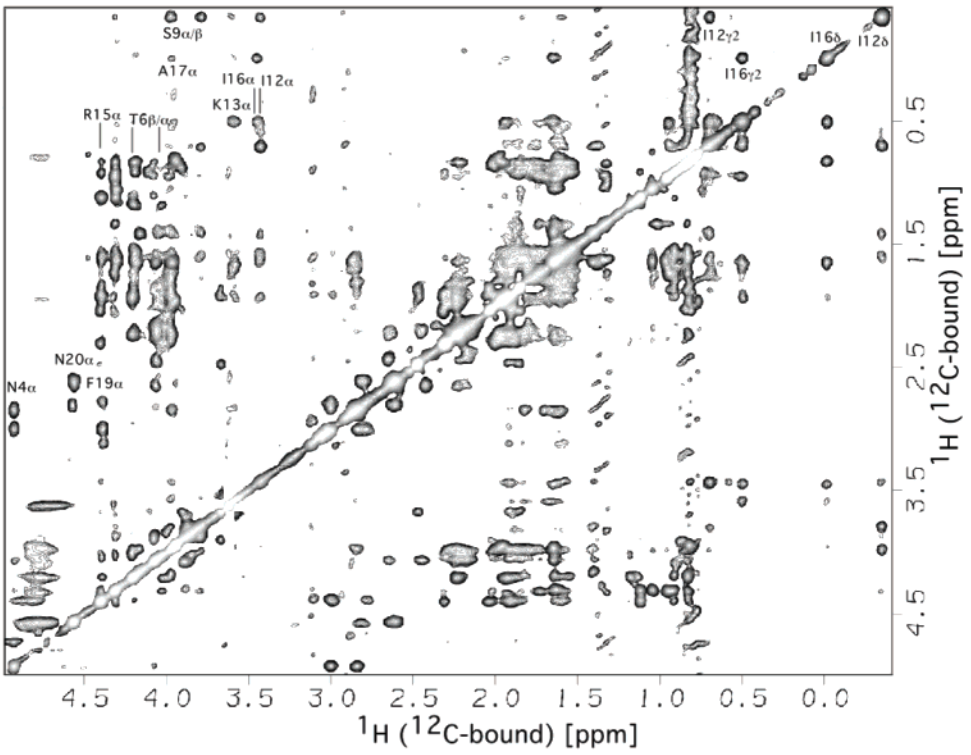

C

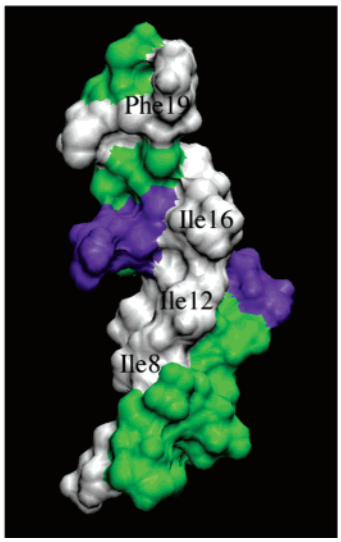

FIGURE 3: Structure of the α-subunit N-terminal peptide in complex with δ′. (A) Secondary structure prediction by PSIPRED (http://bioinf.cs.ucl.ac.uk/psipred/). The confidence of the prediction is indicated above the peptide sequence. H = α helix, and C = coil. The chemical-shift index [CSI (*33*)] is shown for the peptide residues for which α-proton assignment could be obtained. (B) Region of a ^{12}C/^{12}C-edited NOESY spectrum of the δ′−αN complex. Some of the assignments are indicated. (C) Structure of the α-subunit N-terminal peptide in complex with δ′. The diagram in C was generated with VMD (http://www.ks.uiuc.edu/Research/vmd/).

greater than 0.5 Å, and the backbone root-mean-square deviation (rmsd) of the 10 structures (residues 3−20) was 0.57 Å. Figure 3C shows the final derived structure of the α-subunit N-terminal peptide. As can be seen in Figure 3C, the structure shows residues Ile8, Ile12, Ile16, and Phe19 forming a hydrophobic cluster on one face of the α helix, while Leu11 is pointing more toward the backside of the helix, which exposes the polar side chains of residues Asn4, Thr6, Glu7, Glu10, Lys13, Gln14, and Gln18.

Structure of the αN−δ′ Complex from Intermolecular NOEs. Figure 4A shows a region of a ^{13}C/^{12}C-filtered NOESY spectrum (left spectrum) in which NOEs are detected between ^{13}C-bound protons (δ′) and ^{12}C-bound protons (αN). NOEs between δ′ and αN protons were also

Table 1: Resonance Assignments of the α-Subunit N-Terminal Peptide in Complex with the δ-Subunit N-Terminal Domain

	Δppm[a]	α	β1/β2	γ11/γ12/γ2*	δ1/δ2	other
Gln2	−0.7	3.67	1.93/1.87	2.48		
Leu3	0.15	4.32	1.64		0.98/1.07	
Asn4	0.19	4.94	3.03/2.84			
Ser5	−0.41	4.09	3.90			
Thr6	−0.32	4.03	4.2	1.19		
Glu7	0.11	4.4	1.92	2.3/2.03		
Ile8	0.37	4.32	1.75	1.13/0.96	0.84	
Ser9	−0.52	3.98	3.89/3.79			
Glu10	−0.29	4.0	2.02/1.89	2.22		
Leu11	0.02	4.19	1.57		0.84/0.92	
Ile12	−0.51	3.44	1.42	1.62/0.57/0.71	−0.34	
Lys13	−0.77	3.59	1.86			2.86 (ε)
Gln14	−0.31	4.06	2.21	2.67/2.46		
Arg15	0.02	4.4	1.93		3.11/2.94	
Ile16	−0.5	3.45	1.97	1.66/0.84/0.51	−0.02	
Ala17	−0.37	3.98	1.66			
Gln18	−0.16	4.21	1.94	2.25		
Phe19	−0.25	4.41	3.01/2.78		7.08	7.18 (ε), 7.16 (ζ)
Asn20	−0.17	4.58	2.83/2.63			
Val21	−0.01	3.94	1.98	0.83		

[a] Δppm = Deviation of α proton chemical shift from a random coil value.

observed in ^{15}N-edited 3D NOESY−HSQC spectra recorded in H_2O and unedited 2D NOESY experiments recorded in D_2O (right spectrum). From these experiments, intramolecular NOEs to the −0.02 ppm resonance could be observed from δ′ residues Phe18 (ring protons), Asn72 (backbone and side-chain protons), and Gly73 (amide proton). NOEs to the resonance at −0.34 ppm could be observed from Tyr11 (amide proton and ring protons) and Ala14 (amide proton). NOEs to both αN−Ile12 and Ile16 could be observed from δ residues Ala15 and Leu76. These NOEs served as initial input restraints to calculate 10 structural models of the αN−δ′ complex [together with the NOEs for the α-subunit N-terminal peptide (see above) and the NOEs for the N-terminal domain of δ^{2-106} (*9*)]. The energy-minimized average of the initial model was again used to identify additional NOEs, and the final model of the complex was calculated from a total of 53 intramolecular distance restraints. The binding interaction of δ^{2-106} with αN is summarized in parts B and C of Figure 4. On the basis of the observed NOE pattern, peptide residues Ile12 and Ile16 bind in the hydrophobic pocket formed by the side chains of δ-subunit residues comprising helices I and V in such a way that the α-subunit N-terminal helix is oriented parallel to δ-subunit helix I, at an angle of about 45°.

DISCUSSION

There is now a large number of high-resolution crystal structures available for a variety of catalytic sectors of the ATP synthase, which provide detailed information on the structure and interaction of the catalytic subunits α and β as well as the subunits of the central rotor, γ and ε (nomenclature of the bacterial enzyme). The situation is different with regard to the structure of the stator domain, which is composed of subunits *a*, *b*, δ, and a small portion of the α subunit. The main function of the stator domain is to hold the ATPase and proton-channel domains in the correct spatial arrangement for rotational energy coupling to occur. In addition, it has been speculated that the stator might also function to store a portion of the elastic energy released during proton translocation for subsequent use in catalysis (*25*). As of now, only structures of domains of stator subunits have been reported (*9*, *26*, *27*). What is still largely missing is how these structural pieces interact to produce an intact stator domain. Here, we present one piece of the puzzle, namely, the detailed interaction of the N-terminal domain of the δ subunit with the N-terminal 22 residues of the α subunit. It had been known for some time that the N termini of the α subunits were likely involved in δ binding, as indicated for example by protease- and cross-linking experiments (*11*, *14*). The position of the δ subunit at the top of the F_1, near the N termini of the α and β subunits, was directly visualized by immuno-electron microscopy (*10*). Recently, Senior and colleagues showed that a peptide comprising the 22 N-terminal residues of the α subunit was able to bind isolated δ subunit (and δ′) with high affinity, and evidence was presented that the α-subunit N-terminal peptide was helical in solution and that its binding site on the δ subunit was formed by helices I and V (*19*). A more detailed analysis with mutant peptides revealed which residues and what region of the α subunit N terminus were important for tight binding to the δ subunit (*20*). The strongest binding ($K_d \sim 120$ nM) was observed with a wild-type peptide comprising the first 22 residues of the α subunit. Dramatic effects were observed when the conserved, hydrophobic residues involved in binding were changed to charged residues [for example, the point mutation Ile12Glu lead to a complete loss of interaction based on fluorescence assays (*20*)]. This previous work led to a generalized model of how αN might bind in helical form to δ.

The NMR structural data presented here independently verify this model and significantly extend it by providing structural detail. The presence of clearly resolved NOEs between δ- and α-subunit residues indicates that their interaction is specific and that both are in a stable conformation. The deviation of α-proton chemical shifts from random coil values is consistent with an amphipathic α-helical structure of residues 5−20 in the α-subunit N-terminal peptide. Figure 3C shows the structure of the α-subunit N-terminal peptide as it is bound to δ′. The intermolecular NOEs observed between peptide residues Ile8, Ser9, Ile12, Lys13, Arg15, Ile16, Ala17, and Phe19 and δ′ residues Val7, Pro10, Tyr11, Ala14, Ala15, Asn72, Gly73, Asn75, Leu76, and Val79 suggest that the α-subunit N-terminal helix is oriented parallel to helix I of the δ subunit, at an angle of about 45°. This orientation is also consistent with fluorescence-binding experiments conducted with the α-subunit N-terminal peptide containing the Ile16Glu mutation (*20*). Binding of this mutant peptide led to a decrease in fluorescence intensity of the tryptophan residue in the δ-subunit N-terminal domain (δTrp28), in contrast to the increase in fluorescence intensity observed with all peptides containing the wild-type residue Ile16 in this position. Thus, the character of the amino acid in position 16 of the peptide has a pronounced influence on the environment of this tryptophan residue. Parts B and C of Figure 4 summarize the orientation and interactions of the α-subunit N terminus with the δ-subunit N-terminal domain. As noted earlier, these structural interactions achieve a tight complexation between α and δ. Unfortunately, none of the currently available high-resolution X-ray crystallographic models of F_1-ATPase shows electron density for

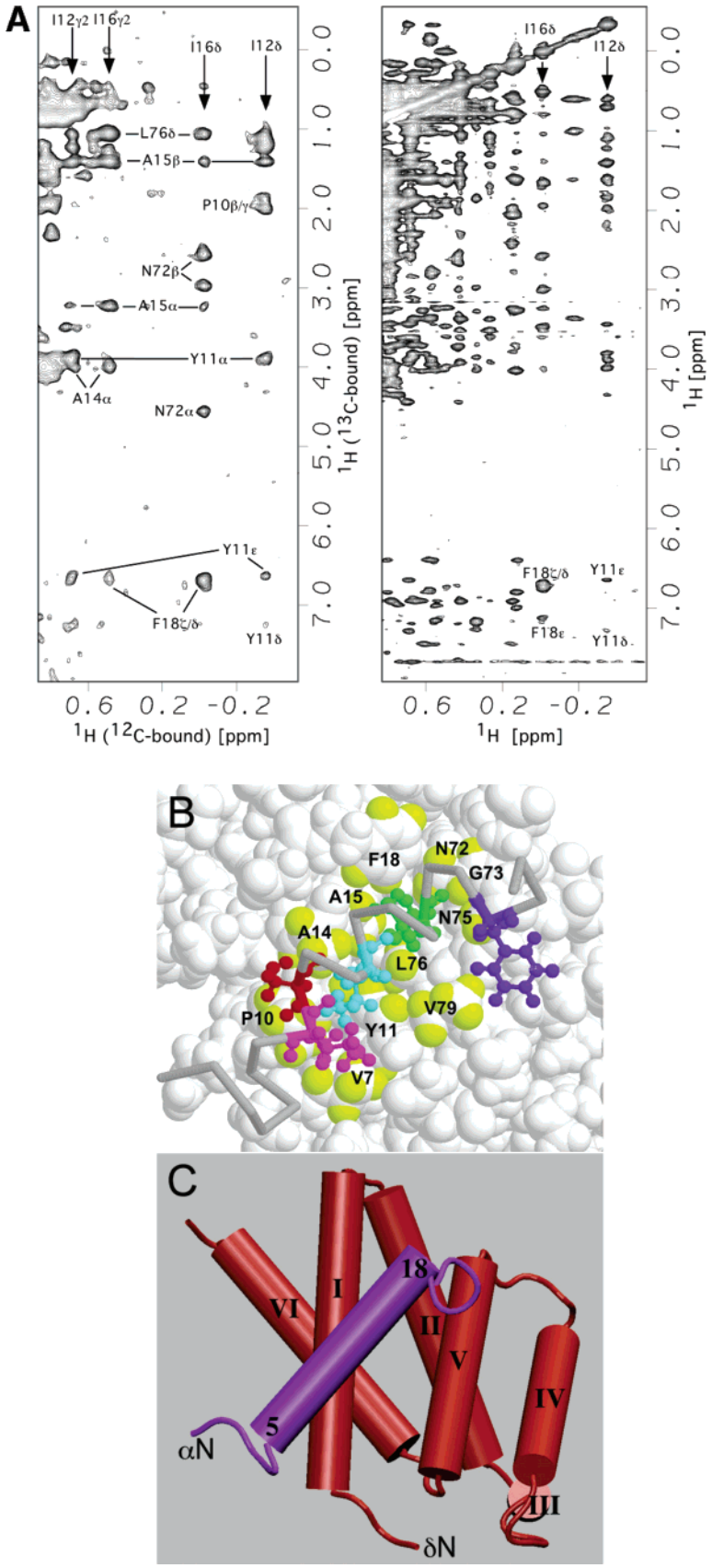

FIGURE 4: Interaction of the α-subunit N-terminal peptide with the δ-subunit N-terminal domain. (A) (Left) Aliphatic region of a ^{12}C/^{13}C-filtered NOESY spectrum of δ′−αN recorded in D_2O. (Right) Same region of an unfiltered NOESY spectrum of δ′−αN. Some of the assignments are indicated. (B) Interaction of αN with δ′. Protons of δ′ residues involved in intermolecular NOEs are in yellow. αN residues Ile8 (magenta), Ser9 (red), Ile12 (cyan), Ile16 (green), and Phe19 (blue) are shown in ball-and-stick models. (C) Orientation of the α-subunit N-terminal helix (blue) in complex with the δ-subunit N-terminal domain (red). The α helix in the final model includes peptide residues 5−18 as determined by PROCHECK (34). The backbone and side-chain rmsd values for the 10 final models was 0.62 and 1.2 Å, respectively [for residues 3−106 (δ′) and 2−21 (αN)].

the N termini of the α subunits (*4*−*8*), indicating that these are flexible in the absence of the *δ* and *b* subunits. It is therefore not possible at this point to predict the orientation of the *δ*-subunit N-terminal domain on the N-terminal domains of the α and *β* subunits of the F_1-ATPase domain.

It should be kept in mind that the here described interaction between the N terminus of α subunit and the N-terminal domain of the *δ* subunit is not the only interaction involved in stator integrity. Other known interactions occur between the C-terminal region of *δ* and the C terminus of the *b* subunit (*18*), between the *b* subunit and F_1 directly (*28*−*30*) and between the *b* subunit and subunit *a* (*31*). It will be interesting to see whether the structural interactions involved are similar to that shown here between α and *δ*.

REFERENCES

1. Senior, A. E. (1988) ATP synthesis by oxidative phosphorylation, *Physiol. Rev. 68*, 177−231.
2. Boyer, P. D. (1997) The ATP synthase−A splendid molecular machine, *Annu. Rev. Biochem. 66*, 717−749.
3. Fillingame, R. H. (1997) Coupling H^+ transport and ATP synthesis in F_1F_0-ATP synthases: Glimpses of interacting parts in a dynamic molecular machine, *J. Exp. Biol. 200*, 217−224.
4. Abrahams, J. P., Leslie, A. G., Lutter, R., and Walker, J. E. (1994) Structure at 2.8 Å resolution of F_1-ATPase from bovine heart mitochondria, *Nature 370*, 621−628.
5. Bianchet, M., Hullihen, J., Pedersen, P. L., and Amzel, M. (1998) The 2.8-Å structure of rat liver F_1-ATPase: Configuration of a critical intermediate in ATP synthesis/hydrolysis, *Proc. Natl. Acad. Sci. U.S.A. 95*, 11065−11070.
6. Shirakihara, Y., Leslie, A. G., Abarahams, J. P., Walker, J. E., Ueda, T., Sekimoto, Y., Kamabara, M., Saika, K., Kagawa, Y., and Yoshida, M. (1997) The crystal structure of the nucleotide-free $\alpha_3\beta_3$ subcomplex of F_1-ATPase from the thermophilic *Bacillus* PS3 is a symmetric trimer, *Structure 5*, 825−836.
7. Groth, G., and Pohl, E. (2001) The structure of the chloroplast F_1-ATPase at 3.2 Å resolution, *J. Biol. Chem. 276*, 1345−1352.
8. Stock, D., Leslie, A. G. W., and Walker, J. E. (1999) Molecular architecture of the rotary motor in ATP synthase, *Science 286*, 1700−1705.
9. Wilkens, S., Dunn, S. D., Chandler, J., Dahlquist, F. W., and Capaldi, R. A. (1997), Solution structure of the N-terminal domain (residues 1−134) of the *δ* subunit of the *Escherichia coli* F_1F_0-ATP synthase, *Nat. Struct. Biol. 4*, 198−201.
10. Wilkens, S., Zhou, J., Nakayama, R., Dunn, S. D., and Capaldi, R. A. (2000) Localization of the *δ* subunit in the *Escherichia coli* F_1F_0-ATPsynthase by immuno electron microscopy: The *δ* subunit binds on top of the F_1, *J. Mol. Biol. 295*, 387−391.
11. Dunn, S. D., Heppel, L. A., and Fullmer, C. S. (1980) The NH_2-terminal portion of the α subunit of *Escherichia coli* F_1-ATPase is required for binding the *δ* subunit, *J. Biol. Chem. 255*, 6891−6896.
12. Häsler, K., Pänke, O., and Junge, W. (1999) On the stator of rotary ATP synthase: The binding strength of subunit *δ* to $(\alpha\beta)_3$ as determined by fluorescence correlation spectroscopy, *Biochemistry 38*, 13759−13765.
13. Maggio, M. B., Parsonage, D., and Senior, A. E. (1988) A mutation in the α-subunit of F_1-ATPase from *Escherichia coli* affects the binding of F_1 to the membrane, *J. Biol. Chem. 263*, 4619−4623.
14. Ogilvie, I., Aggeler, R., and Capaldi, R. A. (1997) Cross-linking of the *δ* subunit to one of the three α subunits has no effect on functioning, as expected if *δ* is a part of the stator that links the F_1 and F_0 parts of the *Escherichia coli* ATP synthase, *J. Biol. Chem 272*, 16652−16656.
15. Lill, H., Hensel, F., Junge, W., and Engelbrecht, S. (1996) Cross-linking of engineered subunit *δ* to $(\alpha\beta)_3$ in chloroplast F-ATPase, *J. Biol. Chem.* 271, 32737.
16. Rodgers, A. J. W., and Capaldi, R. A. (1998) The second stalk composed of the *b*- and *δ*-subunits connects F_0 to F_1 via an α-subunit in the *Escherichia coli* ATP synthase, *J. Biol. Chem.* 273, 29406−29410.
17. Weber, J., Wilke-Mounts, S., and Senior, A. E. (2002) Quantitative determination of binding affinity of *δ*-subunit in *Escherichia coli* F_1-ATPase, *J. Biol. Chem. 277*, 18390.
18. McLachlin, D. T., Bestard, J. A., and Dunn, S. D. (1998) The *b* and *δ* subunits of the *Escherichia coli* ATP synthase interact via residues in their C-terminal regions, *J. Biol. Chem. 273*, 15162−15168.
19. Weber, J., Muharemagic, A., Wilke-Mounts, S., and Senior, A. E. (2003) ATP synthase. Binding of *δ* subunit to a 22-residue peptide mimicking the N-terminal region of α subunit, *J. Biol. Chem. 278*, 13623−13626.
20. Weber, J., Muharemagic, A., Wilke-Mounts, S., and Senior, A. E. (2004) Analysis of sequence determinants of F_1F_0-ATP synthase in the N-terminal region of α subunit for binding of *δ* subunit, *J. Biol. Chem. 279*, 25673−25679.
21. Lee, W., Revington, M. J., Arrowsmith, C., and Kay. L. E. (1994) A pulsed field gradient isotope-filtered 3D ^{13}C HMQC−NOESY experiment for extracting intermolecular NOE contacts in molecular complexes, *FEBS Lett. 350*, 87.
22. Wider, G., Weber, C., Traber, R., Widmer, H., and Wüthrich, K. (1990) Use of a double half-filter in two-dimensional proton NMR studies of receptor-bound cyclosporine, *J. Am. Chem. Soc. 112*, 9015−9016.
23. Breeze, A. (2000) Isotope-filtered NMR methods for the study of biomolecular structure and interaction, *Prog. Nucl. Magn. Reson. Spectrosc. 36*, 323−372
24. Brünger, A. (1992) *X-PLOR (Version 3.1): A System for X-ray Crystallography and NMR*, Yale University Press, New Haven, CT.
25. Cherepanov, D. A., Mulkidjanian, A. Y., and Junge, W. (1999) Transient accumulation of elastic energy in proton translocating ATP synthase, *FEBS Lett. 449*, 1−6.
26. Del Rizzo, P. A., Bi, Y., Dunn, S. D., and Shilton, B. H. (2002) The "second stalk" of *Escherichia coli* ATP synthase: Structure of the isolated dimerization domain, *Biochemistry 41*, 6875.
27. Dmitriev, O., Jones, P. C., Jiang, W., and Fillingame, R. H. (1999) Structure of the membrane domain of subunit *b* of the *Escherichia coli* F_0F_1-ATP synthase, *J. Biol. Chem. 274*, 15598−15604.
28. Weber, J., Wilke-Mounts, S., Nadanaciva, S., and Senior, A. E. (2004) Quantitative determination of direct binding of *b* subunit to F_1 in *Escherichia coli* F_1F_0-ATP synthase, *J. Biol. Chem. 279*, 11253−11258.
29. McLachlin, D. T., Coveny, A. M., Clark, S. M., and Dunn, S. D. (2000) Site-directed cross-linking of *b* to the α, *β*, and *a* subunits of the *Escherichia coli* ATP synthase, *J. Biol. Chem. 275*, 17571−17577.
30. Motz, C., Hornung, T., Kersten, M., McLachlin, D. T., Dunn, S. D., Wise, J. G., and Vogel, P. D. (2004) The subunit *b* dimer of the F_0F_1-ATP synthase: Interaction with F_1-ATPase as deduced by site-specific spin-labeling, *J. Biol. Chem. 279*, 49074−49081.
31. Fillingame, R. H., and Dmitriev, O. Y. (2002) Structural model of the transmembrane F_0 rotary sector of H^+-transporting ATP synthase derived by solution NMR and intersubunit cross-linking *in situ*, *Biochim. Biophys. Acta 1565*, 232−245.
32. Kraulis, P. J. (1991) MOLSCRIPT: A program to produce both detailed and schematic plots of protein structures, *J. Appl. Crystallogr. 24*, 946−950.
33. Wishart, D. S., Sykes, B. D., and Richards, F. M. (1992) The chemical shift index: A fast and simple method for the assignment of protein secondary structure through NMR spectroscopy, *Biochemistry 31*, 1647−1651.
34. Laskowski, R. A., MacArthur, M. W., Moss, D. S., and Thornton, J. M. (1993) PROCHECK−A program to check the stereochemical quality of protein structures, *J. Appl. Crystallog. 26*, 283−291.

BI0510678